Acta Mech 226, 2313–2322 (2015)
DOI 10.1007/s00707-015-1323-5

A. R. Torabi · A. Campagnolo · F. Berto

Experimental and theoretical investigation of brittle fracture in key-hole notches under mixed mode I/II loading

Received: 23 November 2014 / Revised: 4 February 2015 / Published online: 26 February 2015

Abstract The Brazilian disk specimen weakened by a central dumbbell-shaped slit with two key-shaped ends and made of PMMA is employed to perform mixed mode I/II brittle fracture experiments on key-hole notches for various notch lengths and radii and, also, different mode mixity ratios. The load-carrying capacity of the specimen resulting from the test machine at the onset of sudden fracture is theoretically predicted by means of a well-known brittle fracture criterion, namely the local strain energy density criterion. A good agreement is found to exist between the theoretical and the experimental results.

1 Introduction

Different types of cracks can be recognized in components and structures such as macro- and micro-cracks, voids, inclusions, and scratches. They can be produced as a result of loading, manufacturing process, environmental conditions, etc. As is well known, classic fracture mechanics investigates the mechanical behavior of engineering elements damaged by cracks under various loading conditions. Many investigations have been already performed by the researchers on fracture of engineering materials under monotonic and cyclic loading conditions, and the results have been widely published in the literature. For instance, one can refer to Refs. [1–4] for monotonic and cyclic loadings, respectively. About two decades ago, a new branch, called the notch fracture mechanics (NFM), was born inside the classic fracture mechanics. The NFM investigates fracture of notched components. Since brittle fracture is catastrophic, most of the researchers in the NFM have focused their investigations on fracture of brittle and quasi-brittle materials weakened by notches, particularly V- and U-shaped notches.

One of the most well-established criteria in the field of brittle fracture is the strain energy density (SED) criterion. Sih [5] proposed the strain energy density factor (SEDF) for cracked structural elements by taking into account both the SED and the critical distance measured from the crack tip. According to Sih's criterion, brittle fracture happens in a cracked brittle structural component when the SEDF reaches its critical value [5]. By setting a minimum condition on the SEDF, the direction of crack propagation could also be determined [5]. Although Sih's point-wise criterion was proposed for cracked bodies, it became the start point for the other researchers who extended the SED concept to sharp and round-tip notches (sharp and blunt V-notches, U-notches, etc.) by averaging SED over a specified control volume which embraces the notch edge, in order to predict brittle fracture in notched domains under various loading conditions [6–12]. The SED predictions

A. R. Torabi (✉)
Fracture Research Laboratory, Faculty of New Science and Technologies, University of Tehran,
P.O. Box 13741-4395, Tehran, Iran
E-mail: a_torabi@ut.ac.ir
Tel.: +98 21-61 118 572

A. Campagnolo · F. Berto
Department of Management and Engineering, University of Padova, Stradella, S. Nicola 3, 36100 Vicenza, Italy

have been frequently verified by means of the experimental results obtained from testing various materials, specimens, and notches under different loading conditions including mode I and mixed mode I/II [6–13]. Some recent works on the fracture analysis of blunt notches by means of SED are those published in Refs. [14–18]. The SED criterion has been utilized to estimate the maximum load that U-notched Brazilian disk (UNBD) specimens made of coarse-grained polycrystalline graphite could sustain under pure mode I [14], pure mode II [15], and mixed mode I/II [16] loadings. Mode I fracture of blunt V-notches introduced in three different test specimens made of graphite has been also analyzed by means of SED [17]. In some recent researches, the SED criterion has successfully been extended to torsion [19] and compression [20] loadings.

Other than SED, few failure concepts have also been suggested and utilized for predicting fracture in notched structural components. For instance, the point-stress (with different names e.g., the maximum tangential stress; MTS) and the mean-stress concepts have frequently been employed to predict fracture in V- and U-notches under mode I [21–27], mode II [28,29], and mixed mode I/II [30–36] loading conditions. Moreover, the cohesive zone model [37–40], the finite fracture mechanics [41,42], the theory of critical distances [43], and the J-integral [44–50] have been employed for theoretical fracture assessment of sharp and blunt notches.

Some notch features are not fundamentally original, but they are resulting from applying a repairing method to the original notch shapes weakened by crack(s) and damage(s) emanating from the notch border. For example, consider a U-notch damaged by a crack in its border (see Fig. 1). The most common repairing method for this damaged notch is to remove the crack by drilling a hole with the radius normally equal to the crack length. If the crack length is small and larger than the notch tip radius, a key-hole notch will be obtained from the repairing process. Therefore, recent works in the context of the NFM have been focused on fracture assessment of key-hole notches introduced in brittle components [51–55].

Kullmer and Richard [51] published a research paper dealing with brittle fracture in key-hole notches under mixed mode I/II loading. They performed mixed mode I/II fracture tests on compact-tension-shear-notch (CTSN) specimens made of PMMA and measured experimentally the maximum load that each specimen could sustain [51]. The experimental results were successfully predicted by means of a stress-based brittle fracture criterion.

A valuable work has been recently carried out by Lazzarin et al. [52] on brittle fracture of key-hole notches under mixed mode I/II loading. They performed numerous fracture experiments on key-hole notched rectangular graphite plates of various notch radii under mode I and mixed mode I/II loadings. The experimentally obtained fracture loads have been well predicted by means of the SED averaged over the specified control volume which embraces the notch edge.

Torabi [53] made use of the point-stress and the mean-stress criteria to predict the experimental results published in Ref. [52] under mode I loading and found a very good agreement. The mixed mode I/II test results of Ref. [52] have also been predicted successfully in Ref. [54] by means of the two stress-based criteria, namely the key-hole maximum tangential stress (Key-MTS) and the key-hole mean-stress (Key-MS) criteria.

A recent work on brittle fracture of key-hole notches is that published by Torabi and Abedinasab [55]. They have suggested a new version of the Brazilian disk (BD) specimen containing a central dumbbell-shaped slit with two key-shaped ends, called Key-BD specimen, for conducting fracture tests on PMMA at room temperature under pure mode I loading [55]. The static strength of the Key-BD specimens has been well predicted by means of the point-stress and the mean-stress criteria.

In the present research, the Key-BD specimen made of PMMA with various notch radii and different notch lengths is utilized to perform brittle fracture tests at room temperature under mixed mode I/II loading. The experimentally recorded fracture loads are successfully predicted by means of the SED criterion. Supporting

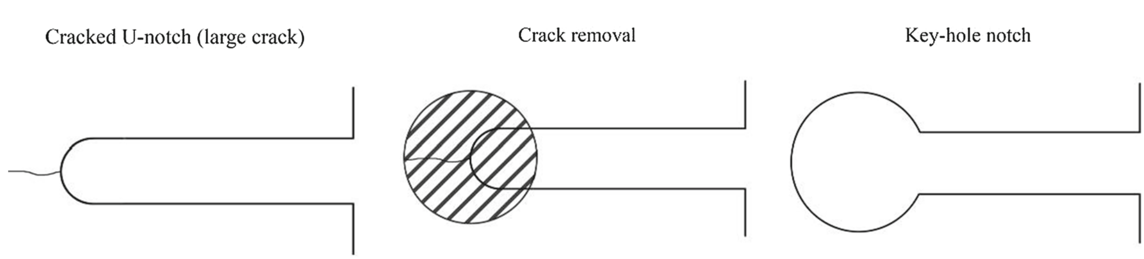

Fig. 1 Key-hole notch resulting from removing a small crack from a U-notch border

Ref. [52], it is demonstrated that SED works well not only on V- and U-notches, but also on key-hole notches of various sizes.

2 Experiments

A new set of brittle fracture tests has been carried out in this research on key-hole notches under mixed mode I/II loading. The material utilized in the experiments is polymethyl-methacrylate (PMMA). PMMA is widely used in typical brittle fracture tests because it is cheap compared to the other brittle materials. The type of PMMA in this study is the same as that reported in Refs. [31,34]. Some of the mechanical properties of the tested PMMA at room temperature are presented in Table 1 [31,34].

The specimen is the same as that reported in Ref. [55], but it is utilized in the present study for testing under mixed mode I/II loading rather than pure mode I loading. As seen in Fig. 2, it is a new version of the well-known Brazilian disk (BD) specimen weakened by a dumbbell-shaped slit with two key-ends, called Key-BD specimen. According to Fig. 2, as the loading angle β (i.e., the angle between the slit bisector line and the loading direction) increases from zero to larger values, various in-plane loading conditions between pure mode I and pure mode II can be achieved. In order to perform fracture experiments under mixed mode I/II loading, the loading angle corresponding to pure mode II loading (β_{II}) should first be determined. For this purpose, a finite element (FE) stress analysis has been performed. Details of determining β_{II} are briefly described herein.

For $\beta = 0°$, the key-ends encounter opening and, hence, they experience pure mode I loading. In this state, the notch bisector line in the vicinity of the notch experiences only the tensile stress. As β increases gradually from zero, the value of tensile stress decreases and, conversely, that of the shear stress increases. For a specific β value, called β_{II}, the tensile stress on the notch bisector line becomes zero meaning that the notch does not experience opening. Trivially, this means pure mode II loading. In other words, to obtain β_{II}, one should increase β from zero till the tensile stresses at the notch bisector line become equal to zero.

The disk diameter (D) and the thickness are equal to 80 and 10 mm, respectively. The slit length (d) is considered to be equal to 24 and 40 mm (the relative notch length ratio RNL d/D is equal to 0.3 and 0.5,

Table 1 Some of the mechanical properties of PMMA at room temperature [31,34]

Material property	Value
Elastic modulus, E (GPa)	2.96
Poisson's ratio, ν	0.38
Ultimate tensile strength (MPa)	70.5
Plane-strain fracture toughness (MPa $m^{0.5}$)	1.96

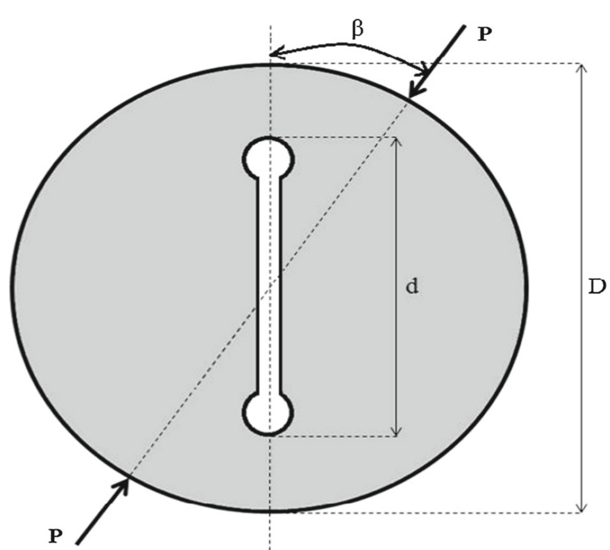

Fig. 2 The key-BD specimen subjected to mixed mode I/II loading

Fig. 3 A key-BD specimen under mixed mode I/II fracture test

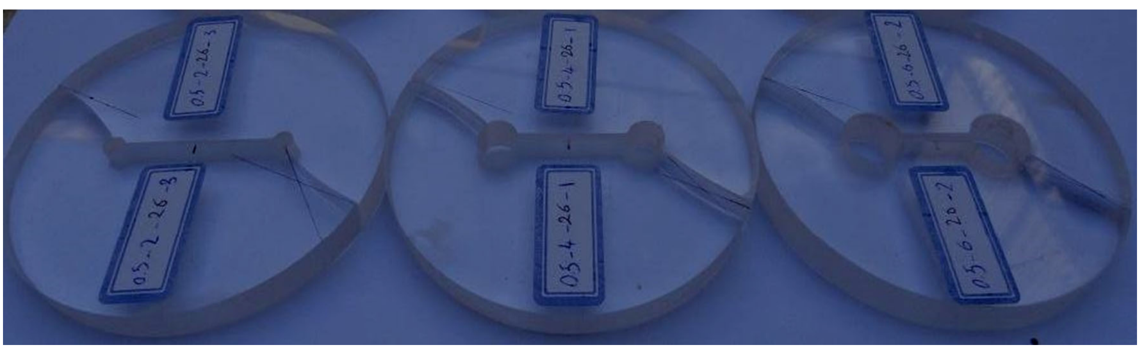

Fig. 4 A few key-BD specimens after fracture

respectively). To produce the Key-BD specimens, a PMMA plate of 10 mm thickness has been first provided, and then, the drawing of each specimen has been submitted to a high-precision 2D CNC water jet cutting machine for fabrication. Finally, the cut surfaces have been accurately polished by means of fine abrasive papers. For the specimens with $d/D = 0.3$, three notch radii of 1, 2, and 4 mm are considered, whereas four radii of 1, 2, 4, and 6 mm for $d/D = 0.5$. The tests are conducted under mixed mode I/II loading conditions. Since β_{II} values are obtained from FE analysis to be equal to approximately 31° and 26° for $d/D = 0.3$ and $d/D = 0.5$, respectively, two values of the loading angle ($\beta = 10$ and 20°, and 10 and 15°) are considered in the tests for the above-mentioned d/D values, respectively. Each test has been repeated three times in order to check the repeatability of the tests. All in all, 42 tests have been performed in the present investigation. In order to provide monotonic loading conditions, the test speed is set to be equal to 0.3 mm/min. Figures 3 and 4 show several Key-BD specimens during and after fracture tests, respectively.

Table 2 summarizes the experimentally recorded fracture loads for different notch radii and various values of the RNL ratio. Each specimen is denoted by a specific index $X - Y - Z$ where X, Y, and Z denote the RNL, the notch radius, and the loading angle β, respectively. For instance, the index 0.3–1–10 identifies the Key-BD specimen with $d/D = 0.3$, having the notch radius of 1 mm, loaded under $\beta = 10°$. Meanwhile, P_i ($i = 1, 2, 3$) denotes the fracture loads for the three tests repeated.

Table 2 The experimental fracture loads of the Key-BD specimens

Specimen index	$P_1(N)$	$P_2(N)$	$P_3(N)$	$P_{av.}(N)$
0.3-1-10	8573	7967	8935	8492
0.3-1-20	8510	8439	8369	8440
0.3-2-10	10,669	9868	10,268	10,268
0.3-2-20	9423	9631	9480	9511
0.3-4-10	9212	9510	9808	9510
0.3-4-20	8599	7965	7332	7966
0.5-1-10	6010	5921	5685	5872
0.5-1-15	5171	5023	5538	5244
0.5-2-10	6991	6835	6679	6835
0.5-2-15	6719	6737	6755	6737
0.5-4-10	7177	7422	7299	7299
0.5-4-15	7109	7109	7109	7109
0.5-6-10	6928	6991	5219	6379
0.5-6-15	6093	5759	6427	6093

The experimental observations have confirmed that the load-displacement plots for the Key-BD specimens are linear up to final breakage. No evidences of large deformations around the notch and abrupt fall of the load from a maximum to zero have confirmed sudden fracture of the specimens. Thus, using brittle fracture criteria for predicting the experimental results is permissible. In the forthcoming sections, the SED averaged over a specified control volume which embraces the notch edge is employed to predict the experimental fracture loads of the Key-BD specimens presented in Table 2.

3 Fracture criterion based on the strain energy density averaged over a control volume

In order to estimate the fracture load of the considered notched structural components, a strain-energy-density based criterion is described in this section by which the fracture loads can be estimated with a reasonable accuracy under mixed mode loading.

Different from Sih's criterion [5], which is a point-wise criterion, the averaged strain energy density criterion, as presented in Ref. [6], states that brittle failure occurs when the mean value of the strain energy density over a given control volume is equal to a critical value, W_c. This critical value varies for different materials but it does not depend on the notch geometry and sharpness. The control volume is thought of as dependent on the ultimate tensile strength and the fracture toughness, K_{Ic}, in the case of brittle or quasi-brittle materials subjected to static loads.

Such a method was formalized and applied first to sharp, zero radius, V-notches under mode I and mixed mode I/II loadings [6] and later extended to blunt U and V-notches [7,8]. Some recent developments and applications are summarized in Refs. [13,56,57].

When dealing with cracks, the critical volume is a circle of radius R_c centered at the tip [6]. Under plane-strain conditions, the critical length, R_c, can be evaluated according to the following expression [6,8]:

$$R_c = \frac{(1+\nu)(5-8\nu)}{4\pi}\left(\frac{K_{Ic}}{\sigma_t}\right)^2 \tag{1}$$

where K_{Ic} is the fracture toughness, ν the Poisson's ratio and σ_t the ultimate tensile strength of a plane specimen that obeys a linear elastic behavior.

For a key-hole notch under mode I, the volume presents the crescent shape shown in Fig. 5a and is defined in Ref. [52], where R_c is the depth measured along the notch bisector line. The outer radius of the crescent shape is equal to $R_c + r_0$, where r_0 depends on the notch opening angle according to the following expression:

$$r_0 = \frac{q-1}{q}\rho \tag{2}$$

with ρ = notch radius and q defined as follows:

$$q = \frac{2\pi - 2\alpha}{\pi}. \tag{3}$$

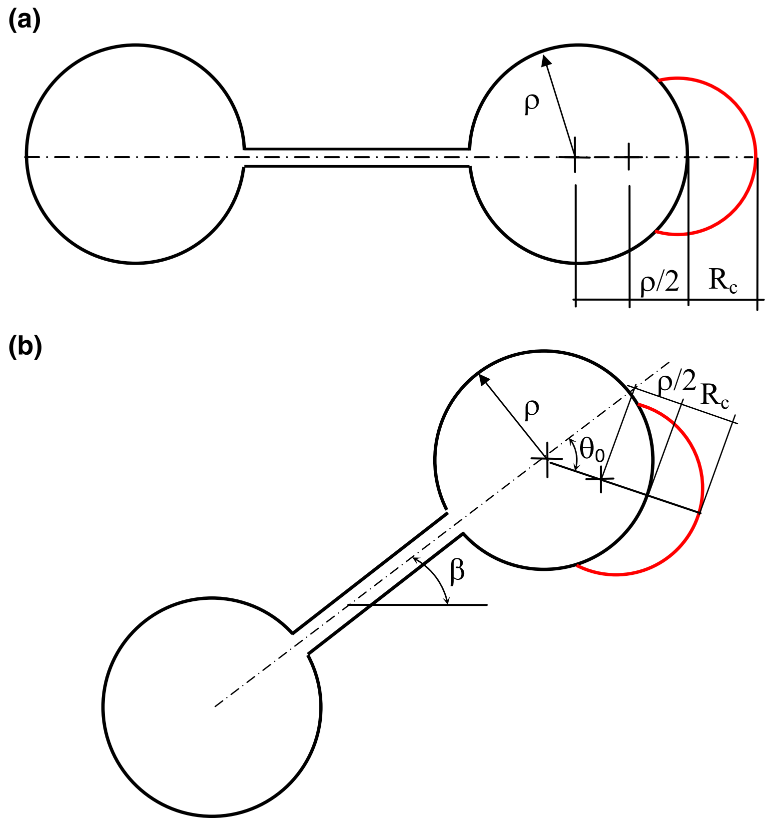

Fig. 5 Control volume under mode I **a** and mixed mode **b** loading for key-hole notched specimens

Under mixed mode loading, the critical volume (see Fig. 5b) is no longer centered on the notch tip, but rather on the point where the principal stress reaches its maximum value along the edge of the notch [9]. It is assumed that the crescent shape volume rotates rigidly under mixed mode, with no change in shape and size. This is the governing idea of the '*equivalent local mode I*' approach, as has been proposed and applied to U and V-notches by Lazzarin et al. [9]. The different size of the control volume under torsion and compression loading with respect to mode I loading has recently been discussed in Ref. [9].

As is discussed above, the idea of the '*equivalent local mode I*' approach, proposed and applied to plates made of PMMA and weakened by U-notches and V-notches [8,9], is used here dealing with key-hole notches under mixed mode I/II loading. With this aim, two models are created for each geometry. The first model is mainly oriented to the determination of the point where the maximum principal stress and the maximum SED are located; the second model is characterized by an accurate definition of the control volume where the strain energy density should be averaged. All the analyses are carried out by using eight-node finite elements under the hypothesis of plane-strain conditions. The procedure to build the two models for determining the SED in the rotated volume can easily be automated by simply writing an ANSYS parametric design language (APDL) subroutine which permits the direct evaluation of the SED in the control volume.

One of the most important advantages of the mean SED approach is the mesh independency [56]. As is widely documented in Ref. [56], refined meshes are not needed, because the mean value of the SED on the control volume can directly be determined via the nodal displacements, without involving their derivatives. As soon as the average SED is known, the notch stress intensity factors (NSIFs) can be calculated *a posteriori* on the basis of very simple expressions linking the local SED and the relevant NSIFs. This holds true also for the stress concentration factors (SCFs), at least when the local stress distributions ahead of the blunt notch are available for the plane problem.

Table 3 Experimental fracture loads compared with theoretical loads evaluated by means of SED

Specimen index	$d/2$	ρ	β	P_1 (N)	P_2 (N)	P_3 (N)	$P_{av.}$ (N)	SED (MJ/m^3)	P_{th} (N)	Δ%		
0.3-1-10	12	1	10	8573	7967	8935	8492	0.944	8010	1.07	0.94	1.05
0.3-1-20	12	1	20	8510	8439	8369	8439	0.969	7858	1.08	1.00	0.99
0.3-2-10	12	2	10	10,669	9868	10,268	10,268	0.965	9582	1.11	0.96	1.00
0.3-2-20	12	2	20	9423	9631	9480	9511	0.990	8762	1.07	1.01	0.99
0.3-4-10	12	4	10	9212	9510	9808	9510	1.127	8209	1.12	1.00	1.03
0.3-4-20	12	4	20	8599	7965	7332	7965	1.317	6361	1.35	1.00	0.92
0.5-1-10	20	1	10	6010	5921	5685	5872	0.987	5416	1.11	1.01	0.97
0.5-1-15	20	1	15	5171	5023	5538	5244	0.990	4829	1.07	0.96	1.06
0.5-2-10	20	2	10	6991	6835	6679	6835	0.952	6420	1.08	1.00	0.98
0.5-2-15	20	2	15	6719	6737	6755	6737	0.917	6447	1.04	1.00	1.01
0.5-4-10	20	4	10	7177	7422	7299	7299	0.972	6786	1.06	1.02	1.00
0.5-4-15	20	4	15	7109	7109	7109	7109	0.966	6628	1.07	1.00	1.00
0.5-6-10	20	6	10	6928	6991	5219	6379	1.115	5537	1.25	1.10	0.82
0.5-6-15	20	6	15	6093	5759	6427	6093	1.133	5245	1.16	0.94	1.06

The SED in the present table has been evaluated applying (in the numerical model) a load corresponding to the average experimental value, being $P = P_{av}$

4 SED approach in fracture analysis of the tested PMMA specimens

The fracture criterion described in the previous section is employed here to estimate the fracture loads obtained from the experiments conducted on the PMMA specimens weakened by key-hole notches under mixed mode loading. The averaged strain energy density criterion (SED) states that failure occurs when the mean value of the strain energy density over a control volume, $\bar{W}$, is equal to a critical value, W_c, which depends on the material but not on notch geometry [6–9]. This critical value can be determined from the ultimate tensile strength σ_t according to Beltrami's expression:

$$W_c = \frac{\sigma_t^2}{2} E. \tag{4}$$

In parallel, the control volume definition via the control radius R_c needs the knowledge of the fracture toughness, K_{Ic}, and the Poisson's ratio, ν, see Eq. (1). The critical load which is sustainable by a notched component can be estimated by imposing $\bar{W}$ equal to the critical value W_c. This critical value is considered here constant under mode I, mode II, and in-plane mixed mode conditions. This assumption has extensively been verified for a number of different brittle and quasi-brittle materials [8].

As is mentioned earlier, the PMMA properties considered in the present investigation are: $\sigma_t = 70.5$ MPa, $K_{Ic} = 1.96$ MPa$\sqrt{\text{m}}$, Poisson's ratio $\nu = 0.38$. As a result, the critical SED for the tested PMMA is $W_c = 0.839$ MJ/m^3, whereas the radius of the control volume is $R_c = 0.166$ mm for plane-strain conditions.

Table 3 summarizes the outlines of the experimental, numerical, and theoretical findings for the tested PMMA specimens, analyzed here by means of SED concepts. In particular, the table summarizes the experimental loads to failure (P), for each notch radius ρ, compared with the theoretical values (P_{th}) based on the SED evaluation. The table also gives us the SED value directly obtained from the FE models of the PMMA specimens.

The last columns of Table 3 report the relative deviations between experimental and theoretical loads ($\Delta = P{*}100/P_{th}$). As is widely discussed in Ref. [8], acceptable engineering values range between −20 and +20 %, being this scatter slightly higher under mixed mode loading or pure mode II loading [9]. As can be noticed from Table 3, this range is satisfied for the majority of the present data with only one exception falling outside the range −20 to +20 %.

The results are plotted also in a graphical form in Figs. 6 and 7 where the *experimental* values of the critical loads (open dots) are compared with the *theoretical* evaluations based on the constancy of the SED in the control volume (solid line). For the notched PMMA specimens with $d/D = 0.5$, the SED against the notch tip radius ρ is shown. The trend of the theoretically evaluated loads is in good agreement with the experimental ones.

A synthesis in terms of the square-root value of the local energy averaged over the control volume (of radius R_c), normalized with respect to the critical energy of the material, against the notch tip radius is displayed in Fig. 8. The plotted parameter is proportional to the fracture load. The new data are plotted together, independent of the notch geometry and specimen shape. The aim is to investigate the influence of the notch tip radius on

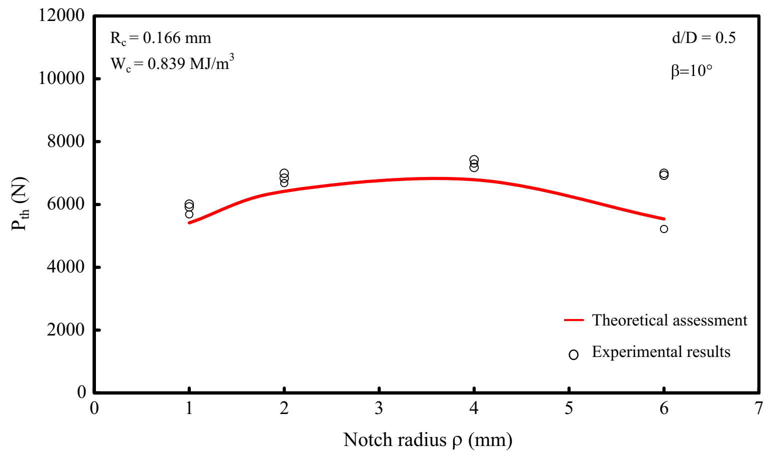

Fig. 6 Fracture assessment by means of SED for the case $d/D = 0.5$ and $\beta = 10°$

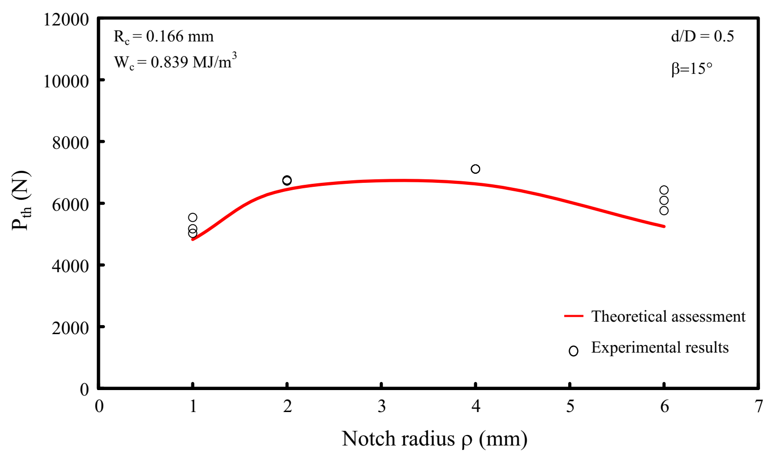

Fig. 7 Fracture assessment by means of SED for the case $d/D = 0.5$ and $\beta = 15°$

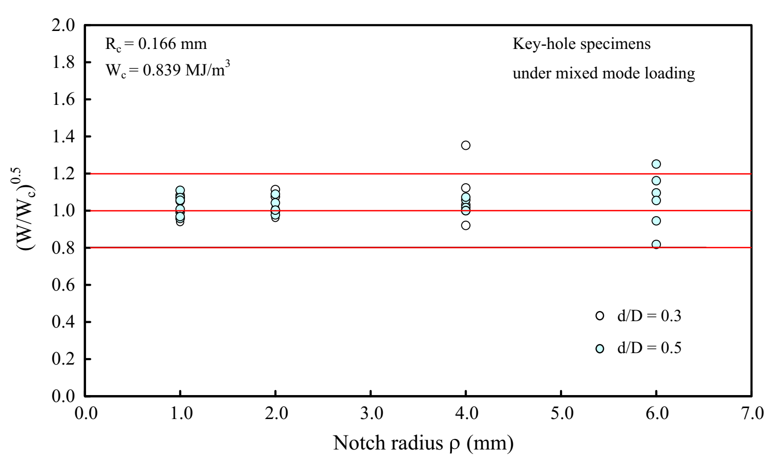

Fig. 8 Synthesis of brittle failure data from PMMA specimens

the fracture assessment based on SED. From Fig. 8, it is clear that the scatter of the data is very limited and almost independent of the notch radius. All the values fall inside a scatter ranging from 0.80 to 1.20, with the majority of the data inside 0.85–1.15 and only two values outside the range from 0.8 to 1.2. The synthesis also confirms the choice of the control volume which seems to be suitable to characterize the material behavior under pure mode II loading. The scatter of the experimental data presented here is in good agreement with the recent database in terms of SED reported in Refs. [8,9].

5 Conclusions

Brittle fracture in key-hole notched PMMA specimens has been investigated both experimentally and theoretically under in-plane mixed mode I/II loading. Fracture tests have been conducted on specimens characterized by different notch geometries, to obtain the fracture loads under the above-mentioned conditions.

The SED criterion is herein applied to rounded-tip key-hole notches in order to estimate the fracture load of notched PMMA components under mixed mode I/II loading. The *equivalent local mode I* concept used in parallel with the SED approach is found to be suitable for the fracture assessment, independent of the loading angle and notch radius.

In the present paper, it is shown that the proposed method is suitable for the PMMA stressed under mixed mode I/II loading conditions, being the experimental loads to failure in good agreement with the results estimated by the SED approach. From the sound agreement between theoretical and experimental results, it can be deduced that for PMMA both the critical energy and the radius of the control volume are constant material properties, at least under in-plane loading being the control radius size determined on the basis of mode I fracture properties. The synthesis also confirms the choice of the crescent shape of the volume which seems to be suitable to characterize the material behavior under mixed mode I/II loading.

References

1. Lauterbach, B., Gross, D.: The role of nucleation and growth of micro cracks in brittle solids under compression: a numerical study. Acta Mech. **159**, 199–211 (2002)
2. Shindo, Y., Narita, F., Sato, T.: Analysis of mode II interlaminar fracture and damage behavior in end notched flexure testing of GFRP woven laminates at cryogenic temperatures. Acta Mech. **187**, 231–240 (2006)
3. Guo, J.H., Lu, Z.X., Feng, X.: The fracture behavior of multiple cracks emanating from a circular hole in piezoelectric materials. Acta Mech. **215**, 119–134 (2010)
4. Brighenti, R., Carpinteri, A., Spagnoli, A.: Influence of material microvoids and heterogeneities on fatigue crack propagation. Acta Mech. **225**, 3123–3135 (2014)
5. Sih, G.C.: Strain-energy-density factor applied to mixed mode crack problems. Int. J. Fract. **10**, 305–321 (1974)
6. Lazzarin, P., Zambardi, R.: A finite-volume-energy based approach to predict the static and fatigue behavior of components with sharp V-shaped notches. Int. J. Fract. **112**, 275–298 (2001)
7. Lazzarin, P., Berto, F.: Some expressions for the strain energy in a finite volume surrounding the root of blunt V-notches. Int. J. Fract. **135**, 161–185 (2005)
8. Berto, F., Lazzarin, P.: Recent developments in brittle and quasi-brittle failure assessment of engineering materials by means of local approaches. Mater. Sci. Eng. R Rep. **75**, 1–48 (2014)
9. Lazzarin, P., Berto, F., Elices, M., Gòmez, J.: Brittle failures from U- and V-notches in mode I and mixed, I + II, mode: a synthesis based on the strain energy density averaged on finite-size volumes. Fatigue Fract. Eng. Mater. Struct. **32**, 671–684 (2009)
10. Ayatollahi, M.R., Berto, F., Lazzarin, P.: Mixed mode brittle fracture of sharp and blunt V-notches in polycrystalline graphite. Carbon **49**, 2465–2474 (2011)
11. Berto, F., Lazzarin, P., Marangon, C.: Brittle fracture of U-notched graphite plates under mixed mode loading. Mater. Des. **41**, 421–432 (2012)
12. Berto, F., Ayatollahi, M.R.: Fracture assessment of Brazilian disc specimens weakened by blunt V-notches under mixed mode loading by means of local energy. Mater. Des. **32**, 2858–2869 (2011)
13. Lazzarin, P., Campagnolo, A., Berto, F.: A comparison among some recent energy- and stress-based criteria for the fracture assessment of sharp V-notched components under mode I loading. Theor. Appl. Fract. Mech. **71**, 21–30 (2014)
14. Torabi, A.R., Berto, F.: Notch fracture toughness evaluation for a brittle graphite material. Mater. Perform. Charact. **3**, 398–413 (2014)
15. Torabi, A.R., Berto, F.: Strain energy density to assess mode II fracture in U-notched disk-type graphite plates. Int. J. Damage Mech. **23**, 917–930 (2013)
16. Torabi, A.R., Berto, F.: Mixed mode fracture assessment of U-notched graphite Brazilian disk specimens by means of the local energy. Struct. Eng. Mech. **50**, 723–740 (2014)
17. Torabi, A.R., Berto, F.: Fracture assessment of blunt V-notched graphite specimens by means of the strain energy density. Strength Mater. **45**, 635–647 (2013)
18. Berto, F., Campagnolo, A., Elices, M., Lazzarin, P.: A synthesis of polymethylmethacrylate data from U-notched specimens and V-notches with end holes by means of local energy. Mater. Des. **49**, 826–833 (2013)
19. Berto, F., Lazzarin, P., Ayatollahi, M.R.: Brittle fracture of sharp and blunt V-notches in isostatic graphite under torsion loading. Carbon **50**, 1942–1952 (2012)
20. Berto, F., Lazzarin, P., Ayatollahi, M.R.: Brittle fracture of sharp and blunt V-notches in isostatic graphite under pure compression loading. Carbon **63**, 101–116 (2013)

21. Ayatollahi, M.R., Torabi, A.R.: Brittle fracture in rounded-tip V-shaped notches. Mater. Des. **31**, 60–67 (2010)
22. Ayatollahi, M.R., Torabi, A.R.: Tensile fracture in notched polycrystalline graphite specimens. Carbon **48**, 2255–2265 (2010)
23. Torabi, A.R.: Fracture assessment of U-notched graphite plates under tension. Int. J. Fract. **181**, 285–292 (2013)
24. Torabi, A.R., Fakoor, M., Pirhadi, E.: Tensile fracture in coarse-grained polycrystalline graphite weakened by a U-shaped notch. Eng. Fract. Mech. **111**, 77–85 (2013)
25. Torabi, A.R.: Estimation of tensile load-bearing capacity of ductile metallic materials weakened by a V-notch: the equivalent material concept. Mater. Sci. Eng. A **536**, 249–255 (2012)
26. Torabi, A.R.: On the use of the equivalent material concept to predict tensile load-bearing capacity of ductile steel bolts containing V-shaped threads. Eng. Fract. Mech. **97**, 136–147 (2013)
27. Torabi, A.R.: Ultimate bending strength evaluation of U-notched ductile steel samples under large-scale yielding conditions. Int. J. Fract. **180**, 261–268 (2013)
28. Ayatollahi, M.R., Torabi, A.R.: Determination of mode II fracture toughness for U-shaped notches using Brazilian disc specimen. Int. J. Solids Struct. **47**, 454–465 (2010)
29. Torabi, A.R., Fakoor, M., Darbani, M.: Pure shear fracture study in a brittle graphite material containing a U-notch. Int. J. Damage Mech. **23**, 839–854 (2013)
30. Ayatollahi, M.R., Torabi, A.R.: A criterion for brittle fracture in U-notched components under mixed mode loading. Eng. Fract. Mech. **76**, 1883–1896 (2009)
31. Ayatollahi, M.R., Torabi, A.R.: Investigation of mixed mode brittle fracture in rounded-tip V-notched components. Eng. Fract. Mech. **77**, 3087–3104 (2010)
32. Ayatollahi, M.R., Torabi, A.R.: Failure assessment of notched polycrystalline graphite under tensile-shear loading. Mater. Sci. Eng. A **528**, 5685–5695 (2011)
33. Ayatollahi, M.R., Torabi, A.R.: Experimental verification of RV-MTS model for fracture in soda-lime glass weakened by a V-notch. J. Mech. Sci. Technol. **25**, 2529–2534 (2011)
34. Ayatollahi, M.R., Torabi, A.R., Azizi, P.: Experimental and theoretical assessment of brittle fracture in engineering components containing a sharp V-notch. Exp. Mech. **51**, 919–932 (2011)
35. Torabi, A.R.: Sudden fracture from U-notches in fine-grained isostatic graphite under mixed mode I/II loading. Int. J. Fract. **181**, 309–316 (2013)
36. Torabi, A.R., Fakoor, M., Pirhadi, E.: Fracture analysis of U-notched disc-type graphite specimens under mixed mode loading. Int. J. Solids Struct. **51**, 1287–1298 (2014)
37. Gómez, F.J., Elices, M.: A fracture criterion for sharp V-notched samples. Int. J. Fract. **123**, 163–175 (2003)
38. Gómez, F.J., Elices, M., Valiente, A.: Cracking in PMMA containing U-shaped notches. Fatigue Fract. Eng. Mater. Struct. **23**, 795–803 (2000)
39. Gómez, F.J., Elices, M.: A fracture criterion for blunted V-notched samples. Int. J. Fract. **127**, 239–264 (2004)
40. Planas, J., Elices, M., Guinea, G., Gómez, F., Cendón, D., Arbilla, I.: Generalizations and specializations of cohesive crack models. Eng. Fract. Mech. **70**, 1759–1776 (2003)
41. Carpinteri, A., Cornetti, P., Pugno, N., Sapora, A., Taylor, D.: A finite fracture mechanics approach to structures with sharp V-notches. Eng. Fract. Mech. **75**, 1736–1752 (2008)
42. Sapora, A., Cornetti, P., Carpinteri, A.: A finite fracture mechanics approach to V-notched elements subjected to mixed-mode loading. Eng. Fract. Mech. **97**, 216–226 (2013)
43. Susmel, L., Taylor, D.: The theory of critical distances to predict static strength of notched brittle components subjected to mixed-mode loading. Eng. Fract. Mech. **75**, 534–550 (2008)
44. Livieri, P.: A new path independent integral applied to notched components under mode I loadings. Int. J. Fract. **123**, 107–125 (2003)
45. Matvienko, Y.U.G., Morozov, E.M.: Calculation of the energy J-integral for bodies with notches and cracks. Int. J. Fract. **125**, 249–261 (2004)
46. Berto, F., Lazzarin, P.: Relationships between J-integral and the strain energy evaluated in a finite volume surrounding the tip of sharp and blunt V-notches. Int. J. Solids Struct. **44**, 4621–4645 (2007)
47. Livieri, P.: Use of J-integral to predict static failures in sharp V-notches and rounded U-notches. Eng. Fract. Mech. **75**, 1779–1793 (2008)
48. Barati, E., Alizadeh, Y., Aghazadeh, J., Berto, F.: Some new practical equations for rapid calculation of J-integral in plates weakened by U-notches under bending. Mater. Des. **31**, 2964–2971 (2010)
49. Barati, E., Alizadeh, Y.: A numerical method for evaluation of J-integral in plates made of functionally graded materials with sharp and blunt V-notches. Fatigue Fract. Eng. Mater. Struct. **34**, 1041–1052 (2011)
50. Becker, T.H., Mostafavi, M., Tait, R.B., Marrow, T.J.: An approach to calculate the J-integral by digital image correlation displacement field measurement. Fatigue Fract. Eng. Mater. Struct. **35**, 971–984 (2012)
51. Kullmer, G., Richard, H.A.: Influence of the root radius of crack-like notches on the fracture load of brittle components. Arch. Appl. Mech. **76**, 711–723 (2006)
52. Lazzarin, P., Berto, F., Ayatollahi, M.R.: Brittle failure of inclined key-hole notches in isostatic graphite under in-plane mixed mode loading. Fatigue Fract. Eng. Mater. Struct. **36**, 942–955 (2013)
53. Torabi, A.R.: Closed-form expressions of mode I apparent notch fracture toughness for key-hole notches. J. Strain Anal. Eng. Des. **49**, 583–591 (2014)
54. Torabi, A.R., Pirhadi, E.: Stress-based criteria for brittle fracture in key-hole notches under mixed mode loading. Eur. J. Mech. A Solids **49**, 1–12 (2015)
55. Torabi, A.R., Abedinasab, S.M.: Fracture study on Key-hole notches under tension: two brittle fracture criteria and notch fracture toughness measurement by the disk test. Exp. Mech. (2014, in press)
56. Lazzarin, P., Berto, F., Zappalorto, M.: Rapid calculations of notch stress intensity factors based on averaged strain energy density from coarse meshes: theoretical bases and applications. Int. J. Fatigue **32**, 1559–1567 (2010)
57. Pook, L.P., Berto, F., Campagnolo, A., Lazzarin, P.: Coupled fracture mode of a cracked disc under anti-plane loading. Eng. Fract. Mech. **128**, 22–36 (2014)